26th ABCM International Congress of Mechanical Engineering
November 22-26, 2021. Florianópolis, SC, Brazil

# EFFECTS OF CORROSION INCIDENCE ON A BIOMASS STEAM GENERATOR UNIT: A CASE STUDY

**Fabiana de Marqui Mantovan**
**Joel Gustavo Teleken**
**Adriana Ferla de Oliveira**
**Eduardo Lucas Konrad Burin**
Federal University of Paraná (UFPR) – Pioneiro Street, 2153, Dallas, Palotina – PR.
e-mail: fabiana.marqui22@gmail.com, joel.teleken@ufpr.br, adrianaferla04@gmail.com and eduardo.burin@ufpr.br

**Edson Bazzo**
Federal University of Santa Catarina (UFSC) – Eng. Agronômico Andrei Cristian Ferreira Street, Trindade, Florianópolis – SC
e-mail: e.bazzo@ufsc.br

**Rafael Welter**
**Cristian Giliard Zapalai**
C-VALE Agroindustrial Cooperative – Ariosvaldo Bitencourt Avenue, 2000, Palotina – PR.
e-mail: rafael.welter@cvale.com.br and cristian.zapalai@cvale.com.br

***Abstract***. *This paper presents the results of a case study whose objective was to evaluate the effects resulting from the incidence of corrosion on the gas side of the heat recovery section of a biomass steam generating unit. The equipment consists on a grate type biomass steam generator with capacity to produce up to 40 t/h of saturated steam (15 bar) and equipped with an economizer and air preheater. During the first four years of operation, the equipment was operated at partial loads (<65% load) and with stoppages on weekends, and during this period a strong development of corrosion was observed in the economizer and air preheater, culminating in the complete degradation of these two components. In this context, the first step consisted of characterizing the biomass used as fuel. Then, the operation of the steam generating unit was monitored based on data obtained from the supervisory system, unburned carbon content in ash, biomass moisture and measurements made with a flue gas analyzer model TESTO 340. The energy diagnosis of the equipment was performed based on the indirect method of the ASME PTC 4 (2013) standard, and the calculations were performed using the Engineering Equation Solver (EES) software. Among the results presented, we highlight the significant reduction in the thermal efficiency of the equipment (-5.0% in relation to the design point condition) caused especially by the presence of air infiltration, partial combustion of the fuel and the absence of pre-heating of the feed water and primary combustion air. The authors suggest, in this context, the importance of monitoring of the elemental composition of the fuel burned, especially with regard to the content of chlorine and sulfur, as well as monitoring the temperatures that occur in the heat recovery section in order to avoid the incidence of moisture condensation on metal surfaces.*

***Keywords:*** *Steam generators, biomass, corrosion, thermal efficiency.*

## 1. INTRODUCTION

The use of air preheater and economizer in the heat recovery section of steam generating units contributes to increase the thermal efficiency of these equipment. However, the heat recovery region is susceptible to increased degradation due to the formation of a corrosive environment that can affect the metal surface of these devices (Alves *et al.*, 2014; Ding *et al.*, 2017; Chen *et al.*, 2017; Suwarno *et al.*, 2021). According to Ebara *et al.* (2013), the control of corrosion in boiler tubes is of great importance, since it affects the efficiency of the equipment and the safety of operators.

The incidence of corrosion in the heat recovery area can occur depending on the concentration of some components in the flue gas. The high sulfur (S) content in fuels, for example, forms sulfur oxides in the flue gases, of which a small portion is sulfur trioxide ($SO_3$). When this combines with water vapor it forms sulfuric acid that condenses on heat transfer surfaces, which in turn leads to corrosion and destruction of surfaces in the low-temperature region (Ganapathy, 1989, Khan *et al.*, 2014, Retschitzegger *et al.*, 2015).

Some works in the literature report the phenomenon of flue gas condensation in industrial scale heat exchangers. The authors Suwarno et al. (2021) analyzed the causes of corrosion in the tubes of an air preheater after five years of operation in a circulating fluidized bed boiler. After the analyses, the authors found that the corrosion of the tubes was caused by acid dew point corrosion, which is caused by the high sulfur and moisture content of the coal. On the other hand, the work

of Alves et al. (2014) reports the factors that led the corrosion of stainless-steel tubes of an air preheater. The results indicated the deposition of chlorides on the internal walls of the tubes (flue gas side), which together with the environment, accelerated the corrosion process.

In general, the presence of corrosion in air preheaters promotes the rupture of the tubes and, as a consequence, the infiltration of air into the flue gas stream. Thus, the amount of air available in the furnace is lower, leading to partial combustion of the fuel and increased concentration of carbon monoxide (CO) in the flue gas. This contributes to increased energy losses associated with the flue gases and incomplete combustion.

The incidence of corrosion can occur not only due to the quality of fuel and flue gas composition, but also due to the operating conditions to meet the steam demand, such as partial load operation and weekend shutdowns. The first condition can represent reduced temperatures in the cold end of flue gas path, while the second causes the thermal stress of metallic structures, due to expansion and contraction of the set in general.

In this regard, the present work performs an energy diagnosis of a biomass steam generator, seeking to analyze the operating conditions adjusted according to the steam demand, always observing the temperature profiles, oxygen content in the heat recovery region and monitoring the quality of the fuel used in the boiler.

## 2. DESCRIPTION OF THE STEAM GENERATING UNIT

This work was conducted using real operating data from a boiler for process steam generation at a poultry and fish processing plant located in the state of Paraná, Brazil.

The biomass (eucalyptus woodchips) steam generator is equipped with a furnace involved with a bundle of finned water tubes connected to the drum firetubes, through which the hot combustion gases pass in two passes. After exchanging heat in the drum, the combustion gases flow to the heat recovery section, where they first pass through the air preheater, transferring heat to the primary air that enters the furnace at a higher temperature than the secondary air, kept at room temperature. Next, the combustion gases pass through the economizer, used to heat the boiler feedwater. Then, the fluegas flow through the multicyclone, where part of the particulate material is retained, and follow the gas path until they reach the stack, where they are released into the atmosphere. Figure 1 shows the structural representation of the boiler, and also identifies the two locations where the flue gas sampling was performed to quantify the air infiltration in the heat recovery section of the equipment.

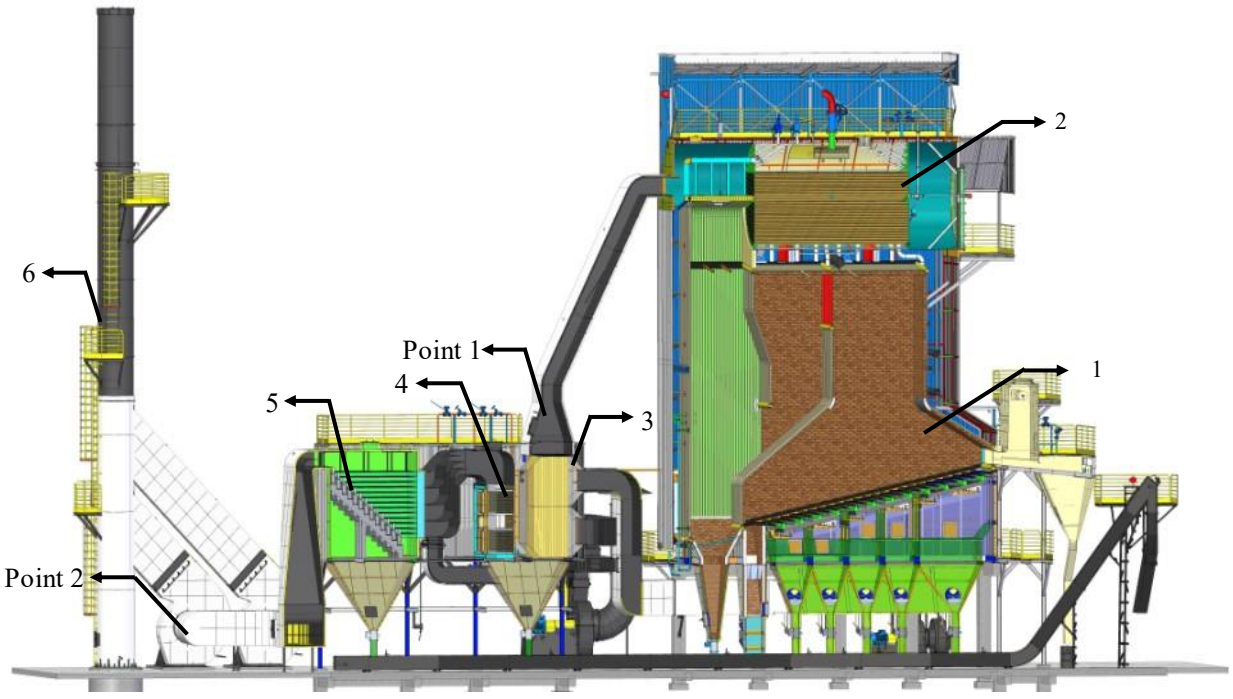


Figure 1. Schematic representation of the steam generator: 1) Furnace; 2) Drum with firetubes; 3) Air Preheater; 4) Economizer; 5) Multicyclone; 6) Chimney; Pont 1) Air preheater inlet. Point 2) Region after the heat recovery section.

In its design condition, the steam generating unit has the capacity to produce 40 ton/h of saturated steam (15 bar). However, due to the production profile of the industrial complex, the boiler was operated with a capacity below 65% load in the first 4 years of operation, with stops on weekends and a working pressure below the design condition. In addition,

after the first 4 years of operation, total deterioration of the air preheater and economizer was observed, requiring the deactivation of these heat exchangers.

In this context, this paper presents preliminary results of an ongoing project that aims to monitor the gaseous and particulate emissions, efficiency and wear off the steam generating unit as a function of the characteristics of the fuel burned. Specifically in this work, the energy diagnosis of the equipment is presented, quantifying energy losses, air infiltration, and also suggesting possible causes for the premature wear off observed in the heat recovery section of the equipment.

## 3. UNIT ENERGY ASSESSMENT

In this work the energy assessment of the steam generating unit was carried out, and three scenarios were considered:

- Project condition: based on design data provided by the equipment manufacturer - adopted as the reference condition;
- Operating condition 1: equipment operated with the economizer deactivated and presence of air infiltration in the air preheater;
- Operating condition 2: equipment operated with economizer and air preheater deactivated, as a way to stop the occurrence of air infiltration until the heat exchangers are replaced.

Due to the steam demand profile of the production process (morning/afternoon: slaughtering; night shift: sanitization of the slaughterhouses), data collection was always performed in the afternoon (runs lasting four hours), and the morning period was considered for stabilization of the boiler's operational parameters.

The methodology adopted for determining the steam generator efficiency was based on the ASME PTC 4 (2013) standard. The standard presents two methods for calculating efficiency, and the one chosen for this work is the indirect method (energy losses method), which allows the identification of energy inputs/outputs in the steam generator's control volume. Eq. (1) represents the formulation of the energy losses method to find the efficiency,

$$\eta_b = \left(1 - \frac{Losses}{Input}\right) 100 \tag{1}$$

where $\eta_b$ is the thermal efficiency of the boiler, *Input* is the energy input [kW] and *Losses* is the sum of all energy losses [kW], calculated as Eq. (2),

$$Losses = L_1 + L_2 + L_3 + L_4 + L_5 + L_6 + L_7 \tag{2}$$

where $L_1$ is the energy loss associated with the flue gases leaving the unit through the stack [kW], $L_2$ is the heat loss associated with the fly ash leaving the unit through the multicyclone [kW], $L_3$ is the heat loss associated with the bottom ash leaving the unit through the furnace [kW], $L_4$ is the loss due to carbon monoxide (CO) content in the flue gas [kW], $L_5$ is the loss related to purges [kW], $L_6$ is the heat loss by radiation and convection at the boiler surfaces [kW] and $L_7$ is the energy loss due to the presence of unburned carbon in the ash [kW].

The energy loss associated with the flue gases leaving the unit ($L_1$) takes into account the loss associated with dry gases from combustion ($L_{gases}$) plus the loss associated with moisture present in the gases ($L_{water}$), as noted in Eq. (3).

$$L_1 = L_{gases} + L_{water} \tag{3}$$

The dry gas energy loss was calculated according to Eq. (4) and the associated moisture loss was calculated according to Eq. (5),

$$L_{gases} = \left(\frac{44}{12} C\, \Delta H_{CO2} + \frac{64}{32} S\, \Delta H_{SO2} + (0{,}7685\, m_{air} + N)\, \Delta HN_2 + e\, m_{air}\, \Delta H_{air}\right) m_{fuel} \tag{4}$$

$$L_{water} = \left(9\, H + H_2O_{fuel} + e\, m_{air}\, \omega\right) \Delta H_{water}\, m_{fuel} \tag{5}$$

where $C$ is the fuel carbon content [kg/kg$_{fuel}$], $\Delta Hco_2$ the $CO_2$ enthalpy [kJ/kg], $S$ the fuel sulfur content [kg/kg$_{fuel}$], $\Delta Hso_2$ the $SO_2$ enthalpy [kJ/kg], $m_{air}$ is the dry stoichiometric air mass flow per kg of fuel [kg$_{air}$/kg$_{fuel}$], $N$ the fuel nitrogen content [kg/kg$_{fuel}$], $\Delta HN_2$ the $N_2$ enthalpy [kJ/kg], $e$ is the air excess, $\Delta H_{air}$ the enthalpy of dry air [kJ/kg$_{air}$], $m_{fuel}$ the fuel mass flow [kg$_{fuel}$/s], $H$ the fuel hydrogen content [kg/kg$_{fuel}$], $H_2O_{fuel}$ the fuel moisture [kg/kg$_{fuel}$], $\omega$ the air absolute humidity [kg$_{water}$/kg$_{air}$] and $\Delta H_{water}$ the water enthalpy[kJ/kg]. All enthalpies were calculated according to the stack temperature and based on the same reference condition [T = 25°C e P = 1 bar]. In case of moisture enthalpy, the latent heat was not considered, once LHV was used in calculations.

The heat loss associated with the fly ash ($L_2$) was calculated according to Eq. (6),

$$L_2 = \Delta H_{ash}\, Fr\, A\, m_{fuel} \quad (6)$$

where $\Delta H_{ash}$ is the enthalpy of ash calculated according to the correlations available in the standard ASME PTC 4 (2013) [kJ/kg$_{ash}$]; $Fr$ is the proportion of fuel ash leaving the multicyclone [$Fr$ = 0,3] and $A$ is the ash content of the fuel [kg$_{ash}$/kg$_{fuel}$].

The heat loss associated with the bottom ash ($L_3$) was also calculated according to Eq. (6), using $Fr$ = 0,7, and assuming the bottom ash temperature of 1100°C, as recommended by the standard for cases where the flow temperature is not measured.

The loss $L_4$ related to the carbon monoxide (CO) content in the flue gas was calculated according to Eq. (7),

$$L_4 = \frac{CO\ \rho\ V_{gases}\ HV_{CO}\ m_{fuel}}{10^6} \quad (7)$$

where $CO$ is the concentration of carbon monoxide in the flue gas [ppm], $\rho$ is the CO density [$\rho$ = 1,25 kg/Nm$^3$], $V_{gases}$ is the volume of dry flue gas per unit mass of fuel burned [Nm$^3$/ kg$_{fuel}$] e $HV_{co}$ is the CO heating value [$HV_{co}$ = 10111 kJ/kg].

To calculate the heat losses related to purges ($L_5$) it is necessary to know the purge flow rate, as well as the frequency and duration of the purging operations (Bazzo, 1995). However, in this work, it was considered that the purge flow corresponds to the percentage of 3% of the steam flow, as reported by Cortes-Rodriguez *et al.* (2016).

Similar analysis was performed for the calculation of radiation and convection losses ($L_6$). In this work it was considered this loss to be equal to 1% of the total energy made available in the furnace in relation to the design condition, within the range suggested by Bazzo (1995).

Finally, in order to estimate the energy loss due to the presence of unburned carbon in the ash ($L_7$), ash samples were collected along each run and the unburned carbon content was determined according to the standard ASTM D1102 (2013). In Eq. (6) is presented the calculation to determine the loss by unburned carbon,

$$L_4 = \frac{C_{unb}\ A}{1 - C_{unb}}\ HV_c\ m_{fuel} \quad (8)$$

where $C_{unb}$ is the unburned carbon content in the ash [kg$_{carbon}$/kg$_{ash}$] and $HV_c$ the carbon heating value [$HV_c$ = 33727 kJ/kg$_{carbon}$].

Table 1. Eucalyptus woodchips properties.

| | Units | Eucalyptus chip |
|---|---|---|
| Proximate analysis | | |
| Ash | (wt %, db[a]) | 0,60 |
| Moisture | (wt %, raw[b]) | 30 - 45 |
| Volatile matter | (wt %, daf[c]) | 84,45 |
| Fixed carbon | (wt %, daf[c]) | 15,55 |
| | | |
| Ultimate analysis | | |
| C | (wt %, daf[c]) | 47,01 |
| H | (wt %, daf[c]) | 7,27 |
| N | (wt %, daf[c]) | <0,02 |
| S | (wt %, daf[c]) | <0,02 |
| O | (wt %, daf[c]) | 45,40 |
| Cl | (wt %, daf[c]) | 0,052 |
| F | (wt %, daf[c]) | <0,0025 |
| | | |
| Lower heating value | | |
| LHV[d] | (MJ kg$^{-1}$, daf[c]) | 18,82 |

[a] Dry basis.
[b] The fuel moisture varied between the range shown.
[c] Dry and ash free.
[d] Lower heating value.

The oxygen ($O_2$) and CO contents in the flue gas were determined using a TESTO 340 flue gas analyzer. The steam generator operational data was collected from the supervisory system and calculations were performed using Engineering Equation Solver (EES) software.

To quantify the air infiltration in the heat recovery section of the unit, flue gas measurements were taken in two regions: at the entrance of the air preheater (Point 1 in Figure 1) and after the heat recovery region (Point 2 in Figure 1). With this, the results found for condition 1 (scenario with part of the air preheater tubes cracked and without economizer) and condition 2 (without air preheater and economizer) were compared with the design condition for energy evaluation of the steam generator.

To characterize the eucalyptus woodchips (fuel) used in the steam generator, the following analyses were performed: proximate analysis (ASTM E870, 2019), ultimate analysis (ASTM D3176, 2015) and heating value (ASTM D5865, 2019). The chloride and fluoride contents were quantified using ion chromatography, following the standards BS EN 14582 (2016) and ASTM D4327 (2017). For moisture analysis of the fuel in natura the standard ABNT 14929 (2017) was used. In Table 1 results are presented.

## 4. RESULTS AND DISCUSSION

The data for design condition and operating conditions 1 and 2 are presented in Table 2. The design condition refers to the values presented by the equipment manufacturer. Operating conditions 1 and 2, in turn, are based on field test data, with the boiler operation adjusted according to the steam demand.

Because of the measurements taken at points 1 and 2 (Figure 1) it was possible to identify significant difference of $O_2$ concentration in the flue gases in operating condition 1. The percentage of $O_2$ found in Point 1 was 3.5%, below the condition established in design by the manufacturer. In point 2, in turn, we observed a percentage of $O_2$ in the flue gas of 11.4%. This difference showed the presence of strong air infiltration in the boiler, indicated not only by the difference in the percentage of $O_2$, but also by the high temperature drop of the flue gases after passing through the air preheater. The flue gas temperature drop is a result of the primary air preheating and also due to the dilution of the flue gases with the infiltrated primary air.

Table 2. Results of design condition and operating conditions 1 and 2.

| | Units | Project condition | Operating Condition 1 | Operating Condition 2 |
|---|---|---|---|---|
| Steam flow | t/h | 40 | 23,7 | 27,3 |
| Steam pressure | bar | 15 | 9 | 9 |
| Steam/fuel (mass flow rate relation) | kg/kg | 3,32 | 3,25 | 3,28 |
| Inlet water temperature | °C | 60 | 74 | 68 |
| Environment air temperature | °C | 25 | 28 | 28 |
| Primary air temperature at the air preheater outlet | °C | 88 | 80(1) | (3) |
| Secondary air temperature | °C | 25 | 28 | 28 |
| Flue gas temperature at the air preheater inlet | °C | 261 | 298 | 186 |
| Flue gas temperature at the economizer inlet | °C | 213 | 150 | 186 |
| Flue gas temperature at the economizer outlet | °C | 150 | 150 | 186 |
| Water temperature at the economizer outlet | °C | 88 | (2) | (2) |
| Flue gas temperature in the chimney | °C | 150 | 150 | 186 |
| $O_2$ air preheater inlet (Point 1) | % | 7 | 3,5 | 8,2 |
| Excess air in the furnace | % | 50 | 20 | 64 |
| $O_2$ in the chimney (Point 2) | % | 7 | 11,4 | 8,2 |
| Excess air in the chimney | % | 50 | 133 | 64 |
| Fuel moisture | % | 39 | 39 | 38,5 |
| Unburned carbon | % | 10 | 10 | 24 |
| CO (in the flue gas) | ppm | 224 | 2552 | 289 |
| LHV(4) | kJ $kg^{-1}$ | 9491 | 9491 | 9587 |
| Primary air input in relation to total air mass | % | 80 | 90 | 80 |
| Secondary air input in relation to total air mass | % | 20 | 10 | 20 |

(1) The primary air preheater was promoting air infiltration.
(2) Boiler without the economizer.
(3) Boiler without the air preheater, primary air entering the boiler at environment temperature.
(4) With ash and moisture.

An inspection in the heat recovery area of the steam generator revealed the presence of air infiltration due to corrosion in the primary air inlet area of the air preheater.

According to Alves *et al.* (2014) The main aggressive agent in the air preheater is the condensation of moisture and acids due to the temperature difference between the flue gases and the atmospheric air to be preheated. The incidence of

condensation on the air preheater promotes a corrosive environment for the metal, reducing the thickness of the tube until it promotes wall rupture. Figure 2 shows the structure of the air preheater with corrosion incidence.

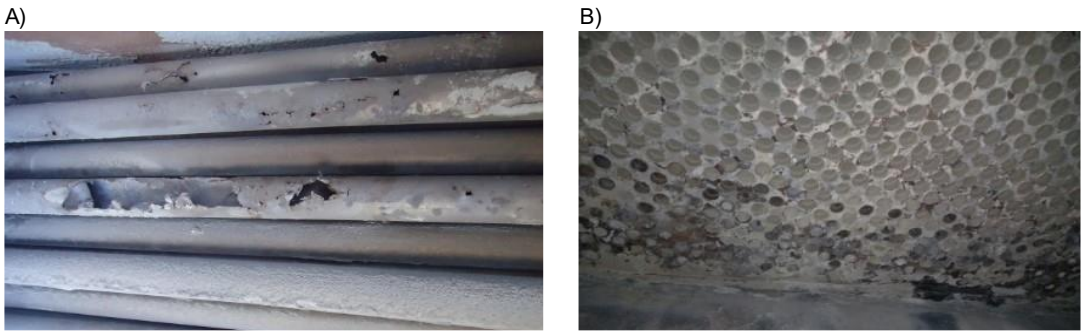


Figure 2. Corroded air preheater tubes: A) Tube wall rupture due to corrosion; B) Evidence of corrosion at the base of the heat exchanger (outlet section of cooled flue gases).

The corrosion related to condensation of moisture and acids is enhanced depending on the composition of the fuel used in the boiler. During the first 4 years of operation, there was no periodic monitoring of the elemental composition of the burned fuel, especially with respect to chlorine and sulfur content. According to literature data (Ebara *et al*., 2013; Alves *et al.*, 2014) these elements can intensify the corrosive attack depending on the atmospheric condition to which they are submitted.

In the work of Frandsen *et al*. (2002) it was found in experiments that metal surfaces subjected to lower temperatures (60ºC) were more vulnerable to severe corrosion compared to surfaces at higher temperatures. Low temperature corrosion is associated with moisture and acid condensation and deposition of hydroscopic salts on the heating surfaces of heat exchangers, whereby these salts contribute to an increase in the dew point of the elements present in the gases (Retschitzegger *et al.*, 2015). Moreover, condensed acids promote the adhesion of particulate material on the heating surface, which usually leads to clogged flow channels (Chen *et al*., 2017).

With the data collected in the field, the thermal efficiency was calculated by the indirect method to evaluate the effects of corrosion on the steam generator. In Figure 3 it is possible to observe the Sankey diagrams for design condition and operating conditions 1 and 2.

As expected, the thermal efficiency of the steam generator in operating condition 1 was lower compared to condition 2 and design condition. With the presence of corrosion, the tubes of the air preheater were ruptured, which increased the concentration of CO in the flue gases ($L_4$). According to Bazzo (1995) the excess air for biomass boilers should be between 30 to 60%. However, the excess of air in the furnace here observed was 20% (Table 2), much lower than the design condition and below the value indicated in the literature. Furthermore, the incidence of air infiltration increased the flow of flue gases, consequently causing an increase in $L_1$ loss by flue gases.

In operating condition 2 the air preheater was by-passed, which contributed to the increase of excess air in the furnace and reduction of CO in the flue gases, as can be seen in Table 2. However, it is observed that the excess air in the furnace needs to be adjusted, because the value is above the design condition, causing an increase in the energy loss in the combustion gases ($L_1$).

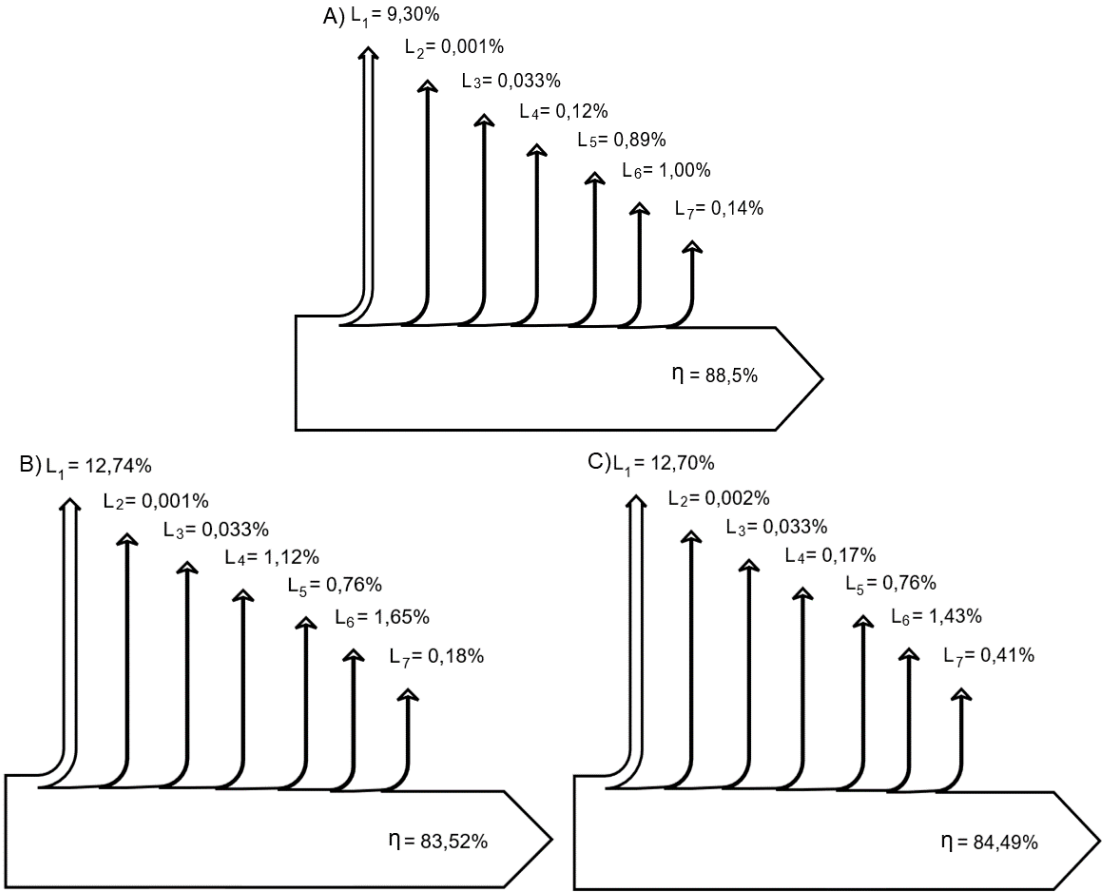


Figure 3. A) Sankey diagram for design condition; B) Sankey diagram for operating condition 1; C) Sankey diagram for operating condition 2.

In Figure 4 it is possible to compare the efficiency of operating conditions 1 and 2 with the design condition and the thermal efficiency curve of the steam generator suggested by the manufacturer.

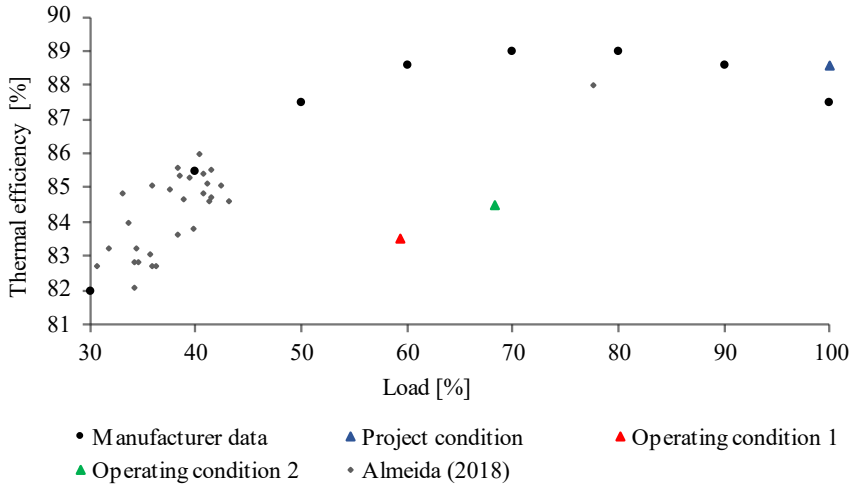


Figure 4. Thermal efficiency of the steam generator.

It can be seen that the design condition dimensioned for eucalyptus chips showed a value close to that established by the manufacturer, indicating consistency in the methodology used. The efficiency of the operation condition 1 is well below the value suggested by the manufacturer, due to the presence of corrosion in the air preheater, causing air infiltration

and incomplete combustion, besides the absence of the economizer, also removed by the deterioration of the metal surface. In operating condition 2 the air infiltration is eliminated. However, the steam generator did not reach the efficiency suggested by the manufacturer, because it was operating without the air preheater and economizer.

The data presented in Figure 4 provided by Almeida (2018) refer to the same steam generator, when it started operating in 2018. In this work, field data was also collected and the thermal efficiency was calculated by the indirect method. Note that the steam generator presented efficiency close to the manufacturer's curve, indicating that at that moment the boiler was in optimal operating conditions.

Making an evaluation of the conditions raised in this work it is possible to infer that some factors may have potentiated the occurrence of corrosion in the heat recovery section, such as: lack of monitoring of the fuel and combustion gases characteristics, control of the temperatures in the heat recovery region in relation to the design condition, weekend shutdowns and boiler operation at partial loads. With this, the heat recovery area was more susceptible to corrosion due to the reduction in gas temperature, culminating in the occurrence of the problems here reported.

## 5. CONCLUSIONS

In general, the incidence of corrosion in the steam generator contributed to significantly reducing the efficiency of the unit and in the deterioration of the heat exchangers in the heat recovery section. In operation condition 1, the presence of corrosion in the air preheater contributed to increase energy losses by incomplete combustion and flue gases, due to air infiltration in the flue gas stream, presenting an efficiency of 83.5%. In contrast, in operation condition 2 the air infiltration was eliminated, due to the total deactivation of the air preheater, increasing the efficiency to 84.5%.

The incidence of severe corrosion was possibly related to the operational conditions (partial loads, stops on weekends), lack of monitoring of the fuel quality, combustion gases and temperature profiles in the heat recovery region. In this regard, it is extremely important to monitor the steam generator, seeking to analyze the operating conditions according to the steam demand and the design conditions, always observing the temperature profiles, oxygen content in the heat recovery region and monitoring the quality of the fuel used in the boiler.

## 6. ACKNOWLEDGEMENTS

The authors acknowledge the Coordination for the Improvement of Higher Education Personnel (CAPES) for the scholarship awarded, the Postgraduation Program in Bioenergy at the Federal University of Paraná (UFPR) and Araucaria Foundation (CP 20/2018 PPP - contract number 047/2020) for the financial support.

## 7. REFERENCES

ABNT 14929, 2017. *Wood — Determination of moisture of chips — Method by drying in oven-dried, ABNT NBR 14929,* Brazilian Association of Technical Standards *ABNT, Rio de Janeiro.*

Almeira, T. G. A., 2018. Thermosolar energy as an alternative for steam and hot water generation in the agro-industrial sector (in Portuguese). Doctoral Dissertation, Graduate Program in Mechanical Engineering, Federal University of Santa Catarina, Florianópolis, Brazil.

Alves, J. O., Saedlou, S. O. B., Oliveira, T. R., 2014. "Piping failure analysis in the air preheater of a sugar mill boiler" (in Portuguese). Technology in Metallurgy Materials and Mining**,** Vol. 11, No. 3, pp. 216-221.

ASME PTC 4, 2013. *Fired Steam Generators - Performance Test Codes, ASME PTC 4 (Revision of ASME PTC 4-2008),* The American Society of Mechanical Engineers ASME, New York.

ASTM D1102, 2013. *Standard Test Method for Ash in Wood, ASTM D1102 – 84 (Reapproved 2013),* American Society for Testing and Materials ASTM, West Conshohocken.

ASTM D3176, 2015, *Standard Practice for Ultimate Analysis of Coal and Coke, D3176 - 15,* American Society for Testing and Materials ASTM, West Conshohocken.

ASTM D4327, 2017, *Standard Test Method for Anions in Water by Suppressed Ion Chromatography, ASTM D4327-17,* American Society for Testing and Materials ASTM, West Conshohocken.

ASTM D5865, 2019, *Standard Test Method for Gross Calorific Value of Coal and Coke, D5865 – 19,* American Society for Testing and Materials ASTM, West Conshohocken.

ASTM E870, 2019, *Standard Test Methods for Analysis of Wood Fuels, E870 − 82 (Reapproved 2019),* American Society for Testing and Materials ASTM, West Conshohocken.

Bazzo, E., 1995. Steam generation (in Portuguese). Publisher of UFSC, Florianópolis.

BS EN 14582, 2016, *Characterization of Waste – Halogen and Sulfur Content – Oxygen Combustion in Closed System and Determination Method,* BS EN 14582 – 16, British Standard European Norm, Brussels.

Chen, H., Pan, P., Shao, H., Wang, Y., Zhao, Q., 2017. "Corrosion and viscous ash deposition of a rotary air preheater in a coal-fired power plant". *Applied Thermal Engineering,* Vol. 113, pp. 373-385.

Cortes-Rodríguez, E. F., Nebra, S. A., Sosa-Arnao, J. H., 2016. Experimental efficiency analysis of sugarcane bagasse boilers based on the first law of thermodynamics. *Journal Of The Brazilian Society of Mechanical Sciences And Engineering*, Vol. 39, No. 3, pp. 1033-1044.

Ding, Q., Tang, X.-F., and Yang, Z. G, 2017. "Failure analysis on abnormal corrosion of economizer tubes in a waste heat boiler". *Engineering Failure Analysis***,** Vol. 73, pp. 129-138.

Ebara, R., Tanaka, F., Kawasaki, M., 2013. "Sulfuric acid dew point corrosion in waste heat boiler tube for copper smelting furnace". *Engineering Failure Analysis*, Vol. 33, pp. 29-36.

Frandsen F., Hansen J., Jensen P. A., Dam-Johansen K., Montgomery M., Fenger L. D., Jensen J. N., Karlsson A., Henriksen N. and Jensen J. P., 2002. "Deposit Formation and Corrosion in the Air Pre-Heater of a Straw-Fired Combined Heat and Power Production Boiler". *IFRF Combustion Journal*, No 200204, pp. 1-23, http://www.journal.ifrf.net/library/may2002/200204frandsen.pdf. Accessed 12 June 2021.

Ganapathy, V., 1989. Cold end corrosion causes and cures. *Hydrocarbon Process*, Vol. 68, pp. 57-59.

Khan, Md. O. A., Damania, S. V., 2014. Corrosion Analysis of Air Pre-Heater Tubes of CFBC Boiler (Slpp) and Improvement in Operation. *International Journal for Scientific Research & Development*, Vol. 2, pp. 854-857.

Retschitzegger, R., Brunner, T., Obernberger, I., 2015. "Low-Temperature Corrosion in Biomass Boilers Fired with Chemically Untreated Wood Chips and Bark". *Energy & Fuels*, Vol. 29, No 6, pp. 3913-3921.

Suwarno, S., Nugroho, G., Santoso, A., Witantyo, 2021. "Failure analysis of air preheater tubes in a circulating fluidized bed boiler". *Engineering Failure Analysis*, Vol. 124, pp. 105380.

Zhai, J.-H., Sun, B.-B.; Zhou, Y., 2021. "Failure analysis on 304 stainless steel tube of semi water gas preheater in coal chemical plant". *Engineering Failure Analysis***,** Vol. 125, pp. 105443.